Biointerphases (2012) 7:37
DOI 10.1007/s13758-012-0037-7

ARTICLE

Assessment of Protein Entrapment in Hydroxyapatite Scaffolds by Size Exclusion Chromatography

Montserrat Espanol · Isidre Casals · Sarah Lamtahri · Maria-Teresa Valderas · Maria-Pau Ginebra

Received: 2 April 2012 / Accepted: 7 May 2012 / Published online: 25 May 2012

Abstract Although it is well known that the textural properties of scaffolds play an important role in the process of tissue regeneration, the investigation of such effects remain difficult especially at the micro/nano level. Texture confers the material the additional ability to entrap/concentrate molecules circulating in the body fluid regardless of their binding affinity to the material. The goal of the present work is to isolate protein entrapment from protein adsorption phenomena in two macroporous hydroxyapatite scaffolds with identical chemical structure, similar macroporosity but different micro/nanoporosity using proteins of different sizes. This was achieved implementing size exclusion chromatography and using the scaffolds as chromatographic columns. The results showed that the larger the crystal size and the lower the packing density of the crystals composing the scaffold increased protein retention but decreased the protein dwelling time in the column. Differences in the amount of protein retained depended on the protein type.

M. Espanol · S. Lamtahri · M.-T. Valderas · M.-P. Ginebra
Department of Materials Science and Metallurgy, Biomaterials, Biomechanics and Tissue Engineering Group, Technical University of Catalonia, Av. Diagonal 647, 08028 Barcelona, Spain

M. Espanol · M.-P. Ginebra (✉)
Center for Research in Nanoengineering, Technical University of Catalonia, Pascual i Vila 15, 08028 Barcelona, Spain
e-mail: Maria.pau.ginebra@upc.edu

M. Espanol · M.-P. Ginebra
Biomedical Research Networking Center in Bioengineering, Biomaterials and Nanomedicine (CIBER-BBN), Maria de Luna 11, Ed. CEEI, 50118 Zaragoza, Spain

I. Casals
Scientific and Technological Centers, University of Barcelona, Luis Sole i Sabaris 1-3, 08028 Barcelona, Spain

1 Introduction

It is currently well acknowledged that upon implantation adsorption of proteins occurs on the surface of biomaterials controlling a variety of biological events like biocompatibility, cell adhesion, immune response and blood coagulation among others [1]. In spite of the importance of these events, protein adsorption is rather a complex system of study not just because of the wide range of proteins that exist in blood, their relative abundance and the fact that adsorption is a dynamic process, but also because the nature of the protein layer at the surface of the material can be easily affected by the characteristics of the underlying material [2–4]. Chemistry, of course, rules the type of protein which would adsorb, but it is in fact the topographical/textural/pore-size features of the material that screen which proteins would have the opportunity to bind upon overcoming the barrier imposed by the nano/micro topography and pore size of the surface. Moreover, topography, besides acting as protein sieve [5], it also favours the retention/concentration of particular proteins within the irregularities of the surface of the material [6]. Therefore, the protein pattern on the surface of a biomaterial should be more accurately regarded as the combination of adsorbed and retained proteins rather than only adsorption events. Probably one of the findings that best proved the importance of retained proteins was the observation in a series of tissue engineering scaffolds of identical chemistry but different architecture that some were osteoinductive while others were not [7–10]. Although the mechanism underlying bone induction is still not fully

known, it is believed that there exists an appropriate geometry that results in the entrapment and concentration of morphogenic/osteogenic proteins responsible for osteoinductivity [10, 11]. In spite of the significance that geometry has in the control of biological events like osteoinductivity, the bottleneck of this research does not come from the lack of materials but from the fact that the gold standard procedure to assess this property is by in vivo assays and this greatly restricts the number of tests [7].

Thus, the motivation of the present work was to develop a method which would help pre-select materials, and more specifically scaffolds for tissue engineering applications, in terms of their ability to concentrate/retain some particular proteins. Having this information one would know how optimum is the architecture of the material at retaining the proteins of interest, how much protein can retain (thus it gives information on the protein dose) and of course, with appropriate tools, one could further assess if the retained protein preserves its conformation which is essential for ensuring biological activity.

Probably the simplest strategy to investigate the entrapment and concentration of proteins within the specific architecture of a material is by chromatography. In broad terms liquid chromatography encompasses a group of techniques which studies the separation of different components in a solution, e.g. proteins, by flushing the solution through a stationary phase with the help of a mobile phase. The hydrodynamic volume [12–14], charge [15], the presence of specific ions or functional groups in a protein [16], the molecule's hydrophobic/hydrophilic character [17, 18], etc. are distinct features in proteins which allow their separation by the various types of chromatographic methods. Most of the existing methods though, are enthalpically driven, thus relying on the affinity (adsorption) of proteins towards the stationary phase and overlooking at the retention/concentration of the proteins as they flow through the stationary phase. Size-exclusion chromatography (SEC) on the contrary, is a chromatographic method in which enthalpic interactions with the stationary phase (adsorption) are minimized, becoming the most suitable method to disclose the protein retention/concentration behaviour dictated by the architecture of the stationary phase. Separation in ideal SEC is entropically driven and is determined solely by the size of the protein in solution (hydrodynamic volume) relative to the size of the pores present in the stationary phase. The movement of the molecules during separation involves random (mass dependent), i.e. diffusion or brownian motion, and the convection (mass independent) movement caused by the flowing of the mobile phase. Hence, in SEC, larger molecules which are unable to enter the smaller pores of the stationary phase will be excluded first (not retained) while the smaller proteins will become more retained and therefore excluded later. This simple theory, implemented in the field of tissue engineering (TE) might help elucidate the most suitable architecture of a scaffold in terms of its ability to retain specific proteins.

Thus the goal of the present work was to apply SEC on stationary phases made of macroporous hydroxyapatite (mHA) scaffolds with a definite architecture. The preparation route that was followed was via a cementitious reaction. This reaction gives an end product which closely resembles the mineral phase of bone (calcium deficient hydroxyapatite) and also allows changes on the nano/micro architecture to be made very easily [19]. The weakness of calcium phosphate cements (CPC) though, is the lack of macroporosity, a point which is essential in the tissue engineering field to allow bone ingrowth. This problem was solved by foaming the liquid phase of the cement by previous incorporation of a surface active molecule that acted as foaming agent [20]. Thus, the architecture of two macroporous HA, with identical composition, similar interconnected macroporosity, and different microstructure was evaluated using three model proteins of acidic isoelectric point but different size: β-lactoglobulin (β-LG) of $\sim$18 kDa, albumin (BSA) of $\sim$66 kDa and γ-globulin (γ-G) of $\sim$150 kDa.

2 Materials and Methods

2.1 Preparation and Characterization of the Macroporous Hydroxyapatite Scaffolds

The preparation of the macroporous hydroxyapatite (mHA) scaffolds was accomplished by mixing a foamed liquid phase with α-tricalcium phosphate powder (α-TCP) in the following manner: (1) First, 2 ml of an aqueous solution which consisted in a 2.5 w/v % of Na_2HPO_4 (Merck, Darmstardt, Germany) and 1 w/v % of Polysorbate 80 (Sigma-Aldrich, St. Louis, USA) was foamed with a domestic food mixer for 30 s at 11,000 rpm; (2) next, one gram of the foam was weighted on a weighing plate onto which the α-TCP powder containing a 2 w% of precipitated hydroxyapatite (Merck, Darmstardt, Germany) was previously spread and both, foam and powder, were carefully mixed with the help of a spatula for 30 s, (3) upon mixture, the foamed paste was either cast into Teflon moulds of 6 mm height and 6 mm diameter or directly injected into Nylon 6 tubes (LEGRIS tubepack®, France) of 50 mm length and 4 mm internal diameter, (4) finally the moulds and tubes were allowed to set in water at 37 °C for 14 days to ensure completion of the hydrolysis reaction. The hydrolysis reaction can be written as follows [21]:

$$3Ca_3(PO_4)_{2(s)} + H_2O_{(l)} \rightarrow Ca_9(HPO_4)(PO_4)_5(OH)_{(s)} \quad (1)$$

In order to obtain mHA scaffolds with different architectures at the micro and nano level, two α-TCP powders with different particle size were used: coarse (C) with a median size of 5.2 μm and fine (F) of 2.8 μm. The α-TCP was in-house made and the preparation protocol can be found in literature [19]. The milling protocol was slightly modified from [19] to achieve the abovementioned sizes. More specifically, the C powder was obtained milling 150 g of powder in a planetary ball mill (Pulverisette 6, Fritsch, Germany) for 15 min at 450 rpm with 10 agate balls of 30 mm diameter and, the F powder by milling for 60 min at 450 rpm and 40 min at 500 rpm with the 10 agate balls of 30 mm diameter and this was followed by a milling of 60 min at 500 rpm with 100 agate balls of 10 mm diameter. To allow comparison between the microstructure of the mHA-F and mHA-C scaffolds, the macro-architecture of both foamed cements was kept similar by adjusting the liquid to powder ratio (L/P) of the cement formulation to 0.55 and 0.65 ml/g for the C and F cements respectively.

With regards to characterization of the foamed HA scaffolds, they were assessed by various techniques. X-ray diffraction analyses (XRD) were performed on previously crushed samples in a PANalyticalX'Pert PRO MPD Alpha1 (Almelo, The Netherlands) system to check for completion of the hydrolysis reaction. The diffractometer equipped with a CuKα X-ray tube was operated at 45 kV and 40 mA. Data were collected in 0.017° steps over the 2θ range of 4°–100° with a counting time of 50 s per step.

A field-emission scanning electron microscope (FE-SEM, Jeol JSM-7001F, Tokyo, Japan) was used to investigate the microstructure of the cross section of the scaffolds. Before observation the scaffolds were Pt/Pd sputtered to minimize charging effects.

Specific surface areas (SSA) of the scaffolds were determined from the nitrogen adsorption data in the relative pressure range (P/P_0) from 0.05 to 0.35 by using the Brunauer-Emmett-Teller (BET) method with the ASAP 2020 physisorption analyzer (Micromeritics, Norcross, GA, USA).

The porosity content and pore size distribution within the material was measured using a mercury intrusion porosimeter (MIP, Autopore IV 9500 Micromeritics, Norcross, GA, USA) with intrusion pressure varied from 5 to 33,000 psi. MIP analyses included assessing the mHA as well as control cements (HA) which were prepared exactly in the same way as the mHA but without the foaming step. The control samples, with identical porosity at the micro level than the mHA [20], were measured because they give more reliable data on the porosity content and pore distribution at the micro/nano level (<1 μm) than the analogous foamed cements.

2.2 Macroporous Hydroxyapatite Analyses by Size-Exclusion Chromatography

Size-exclusion chromatography analyses were performed on a Waters 600 system (Milford, MA, USA) operating at room temperature. The analyses were performed on the 50 × 4 mm Nylon 6 columns filled with either mHA-F or mHA-C (stationary phase). Glass microfiber filters with retention capability down to 1.2 μm (GF/C Whatman, Kent, England) were used as frits and placed on top and bottom of the columns to prevent contamination of the system. Various mobile phases were used on independent columns in order to discriminate adsorption versus retention events. Thus, in some cases the mobile phase consisted in a 30:70 v/v mixture of acetonitrile (ACN, St. Louis, MO, USA) with either 0.1 or 0.4 M ammonium acetate (AA, Scharlau, Barcelona, Spain) and in other cases of a 30:70 v/v mixture of acetonitrile with Milli Q water (18 M cm). All reagents used were of HPLC grade and the solutions prepared were filtered before used. The volume of sample injected was set to 40 μl and its elution was monitored with a Waters 486 UV–Vis tunable wavelength spectrometer (Milford, MA, USA) with 8 μl flow cell at 280 nm. All analyses were performed at a constant flow rate of 0.2 ml/min unless stated otherwise.

For successful disclosure of the exclusion behaviour of the proteins through the columns the following protocol was developed: (1) first, the column was equilibrated with the mobile phase, (2) next, the column was saturated with the protein/s of interest by successive injections of 40 μl of sample at a flow rate of 0.1 ml/min (to maximize protein adsorption) till the eluted amount equalled the injected amount, (3) the column was subsequently rinsed by increasing the ACN content to 100 % over 5 min, was then kept at 100 % ACN flow for 10 min and afterwards the composition of the mobile phase was brought to the initial condition (30:70 ACN:water) in 3 min where it was kept for another 4 min and (4) the sample, i.e. 40 μl of 3–10 mg/ml of a particular protein/s, was injected into the column, carried by the mobile phase through the column to the detector where it was continuously monitored. Step 3 and 4 were repeated for at least 3 times to assess column repeatability and, unless noted differently, the injection of each protein was preceded by saturation with that particular protein. A blank of the column was also performed by injecting mobile phase instead of protein solution and the resulting chromatogram was subtracted from the results. It is noteworthy to highlight that the most important step of the protocol was the rinsing cycle. The small size of the columns to which we were limited to in the present work required of this additional step to visualize the various exclusion events as independent peaks. Without rinsing, the dwelling time of the proteins in the column becomes

too short to allow protein to diffuse into the smaller pores of the stationary phase thus causing the protein to elute as a single broad peak. The rinsing gradient with ACN is believed to enrich the smaller pores with ACN and owing to the lower viscosity of ACN as compared to that of the mobile phase facilitates diffusion of the protein into the pores allowing their separation.

Protein recoveries were calculated from the area under the peaks using the Empower2 software from Waters. Complete recovery was calculated from individual injection of the proteins using a low-dead volume connector instead of the column.

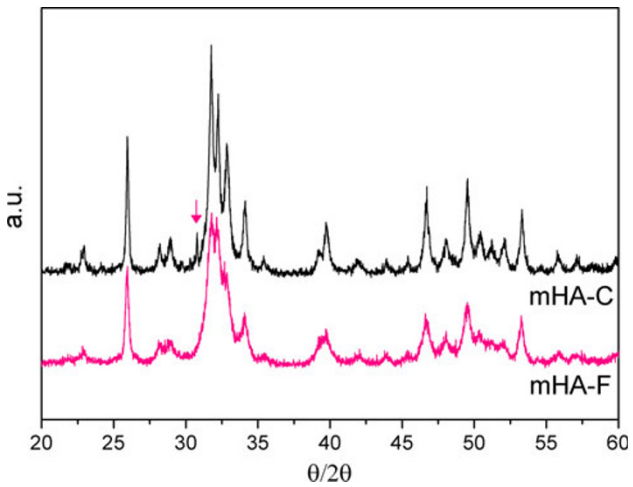

Fig. 1 XRD patterns of the two macroporous cements, i.e. mHA-C and mHA-F. Non labelled *peaks* in the XRD pattern correspond to the HA phase. The *arrow points* to the presence of non-reacted α-TCP

The proteins used for the experiments were bovine serum albumin (BSA), γ-globulin (γ-G) from bovine blood and β-lactoglobulin (β-LG) from bovine milk (Sigma-Aldrich, St. Louis, MO, USA). All proteins were solubilized in Milli Q water, filtered through 0.22 μm mesh filters (MILLEX® GP) and their concentrations measured at 280 nm by means of the Nanodrop ND-1000 (Wilmington, DE, USA) spectrophotometer. All solutions were stored at 2–8 °C when not in use.

3 Results

3.1 Characterization of the Macroporous Hydroxyapatite Scaffolds

Figures 1–3 summarize the main structural features obtained for the two macroporous calcium phosphate scaffolds, i.e. mHA-F and mHA-C. Analyses by XRD (Fig. 1) showed that both materials had identical composition which mostly fitted to hydroxyapatite (JCPDS 9-432) with the exception of a few peaks of much lower intensity (please refer to the arrows in the graph) which were assigned to unreacted α-TCP (JCPDS 9-348). Observation of the surface cross-section of the materials (Fig. 2a, b) revealed a similar macrostructure evidenced by the presence of the macropores introduced by the foaming process. Within the macropores there were openings of varying sizes which allow interconnection with neighbouring macropores. Comparison between F and C scaffolds at the macro level did not show significant differences as both,

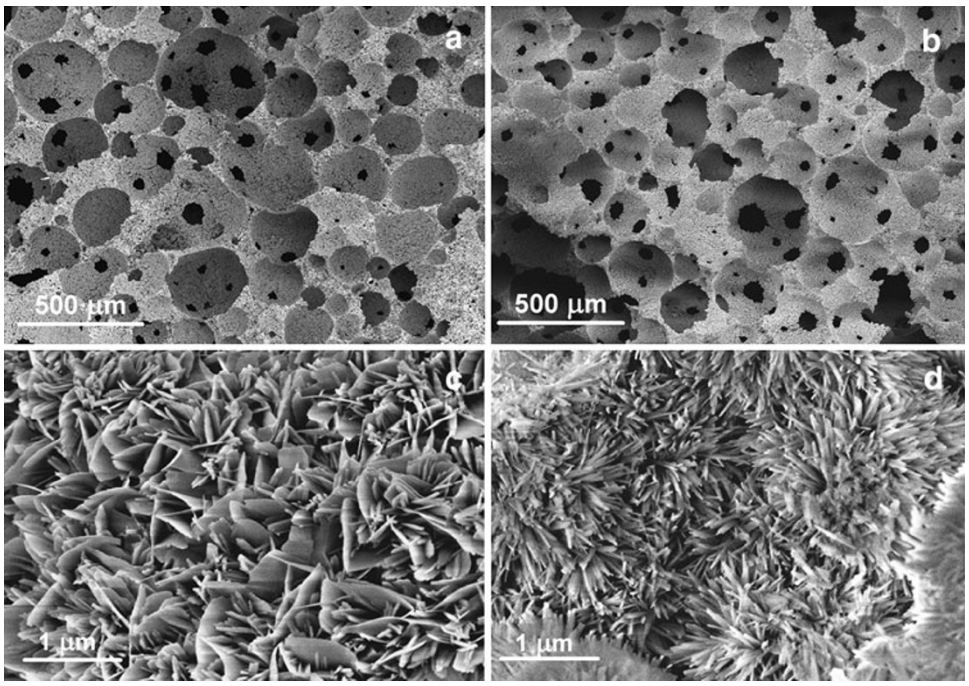

Fig. 2 FE-SEM microstructure for the mHA-C (**a**, **c**) and mHA-F (**b**, **d**) samples revealing the topography of the materials at low (**a**, **b**) and high (**c**, **d**) magnification

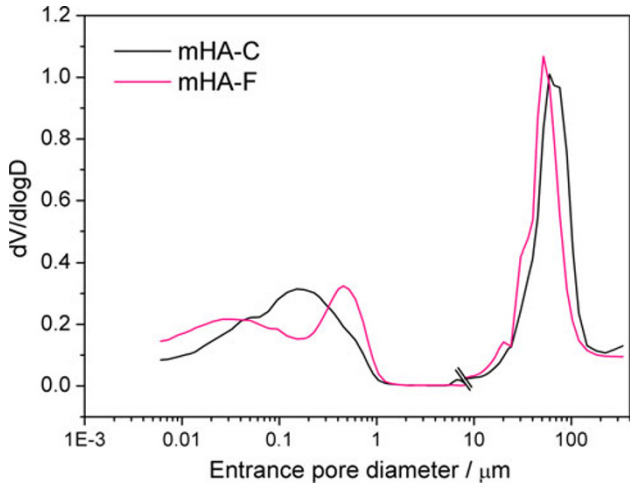

Fig. 3 Pore size distributions obtained from MIP analysis of the mHA-C and mHA-F samples

the size of macropores and openings were comparable. Nevertheless, a close look at the wall structure of both scaffolds clearly exposed differences at the micro level (Fig. 2c, d). The mHA-C scaffold was built by an entangled network of large needle/platy-like crystals which contrasts with the smaller needles observed in the mHA-F scaffold. Furthermore, as the smaller needles in F can be packed more efficiently than the larger crystals in C; the density of crystals was higher in the F scaffold than the C one. These differences were supported by the values in specific surface area measured in both materials: 15.63 ± 0.03 m^2/g for the C scaffold and 35.39 ± 0.10 m^2/g for the F one. Similarly, the MIP results in Fig. 3 summarize in a more quantitative manner the above results: on the one hand, the interconnected pores introduced by the foaming process were indeed of similar size for the F and C scaffolds and were centred around 80 μm and, on the other hand, the differences in crystal size and packing density generated differences in pore size distribution at the nano/micro level (<0.05 μm) resulting in a higher density of smaller pores in the F than the C scaffold.

3.2 Size Exclusion Chromatography Analyses on the Macroporous Hydroxyapatite Scaffolds

In Fig. 4 are compiled the SEC results from injection of the three different proteins, i.e. γ-G, BSA and β-LG, through the mHA-F and mHA-C columns. As can be seen from Fig. 4a, c, e all chromatograms were characterized by two peaks. In SEC, the presence of these two peaks preceded by the injection of a single protein indicates that the protein travels through the column by two different path lengths. There was a first narrow peak that resulted from the quick exclusion of most of the proteins during the first 5 min, and a second exclusion peak which appeared at later times and was of much lower intensity and broader than the first one (please refer to Table 1 for quantitative values). Unlike the first peak, which clearly overlapped in all chromatograms independent of the protein and column, the second peak appeared at different times depending on the type of protein and column. The elution time decreased with protein size: γ-G (150 kDa) eluted first, BSA (66 kDa) second and β-LG (18 kDa) third. Furthermore, proteins eluted faster from the mHA-C column than from the mHA-F one. It was also noteworthy the fact that in the mHA-F column there were less proteins eluting through the second peak (refer to Table 1) and that they dwelled longer time in the column than in the mHA-C column. Another striking result was that all the injected BSA and γ-G eluted completely but, a 30–40 % of the injected β-LG did not elute neither from the C nor from the F column (refer to Table 1). Please note that the peaks centred around 25 min in the β-LG chromatograms and 28 min for the γ-G ones were not the result of size exclusion effects. Their appearance was linked to the protein injections history, i.e. the protein injection sequence which was followed (data not shown), and the peaks probably emerged as the result of protein desorption events.

To confirm that the separation events were of exclusion nature and not from other forms of separation like ion exchange or affinity separation, the elution of the proteins was further investigated on mHA-C columns using mobile phases of different ionic strength: Milli Q water, 0.1 M AA, or 0.4 M AA combined with ACN (70:30 v/v). Figure 5 summarizes the results pertaining to the elution of the various proteins in either Milli Q water or 0.1 M AA combined with ACN. Since the elution profile and the order of elution did not vary with the ionic strength of the mobile phase (AA versus water) one could conclude that the main process governing separation was indeed size exclusion. Investigation of the elution of BSA using 0.1 M AA or 0.4 M AA combined with ACN gave an almost identical profile (data not shown) proving once again that the prevailing mechanism was size exclusion. Furthermore, the similarity in the chromatograms plotted in Fig. 6 corresponding to the elution of γ-G from columns previously saturated with either γ-G or BSA proves that the protein eluted is a fraction of the injected protein and is not the result of desorption from the column reinforcing that the mechanism underlaying separation is not via adsorption–desorption events.

4 Discussion

The awareness that biological events like osteoinduction can be influenced and even controlled by the architecture of a scaffold, has made the geometry of materials to become a discriminatory point in the selection of materials for applications in areas like bone regeneration. Not all the

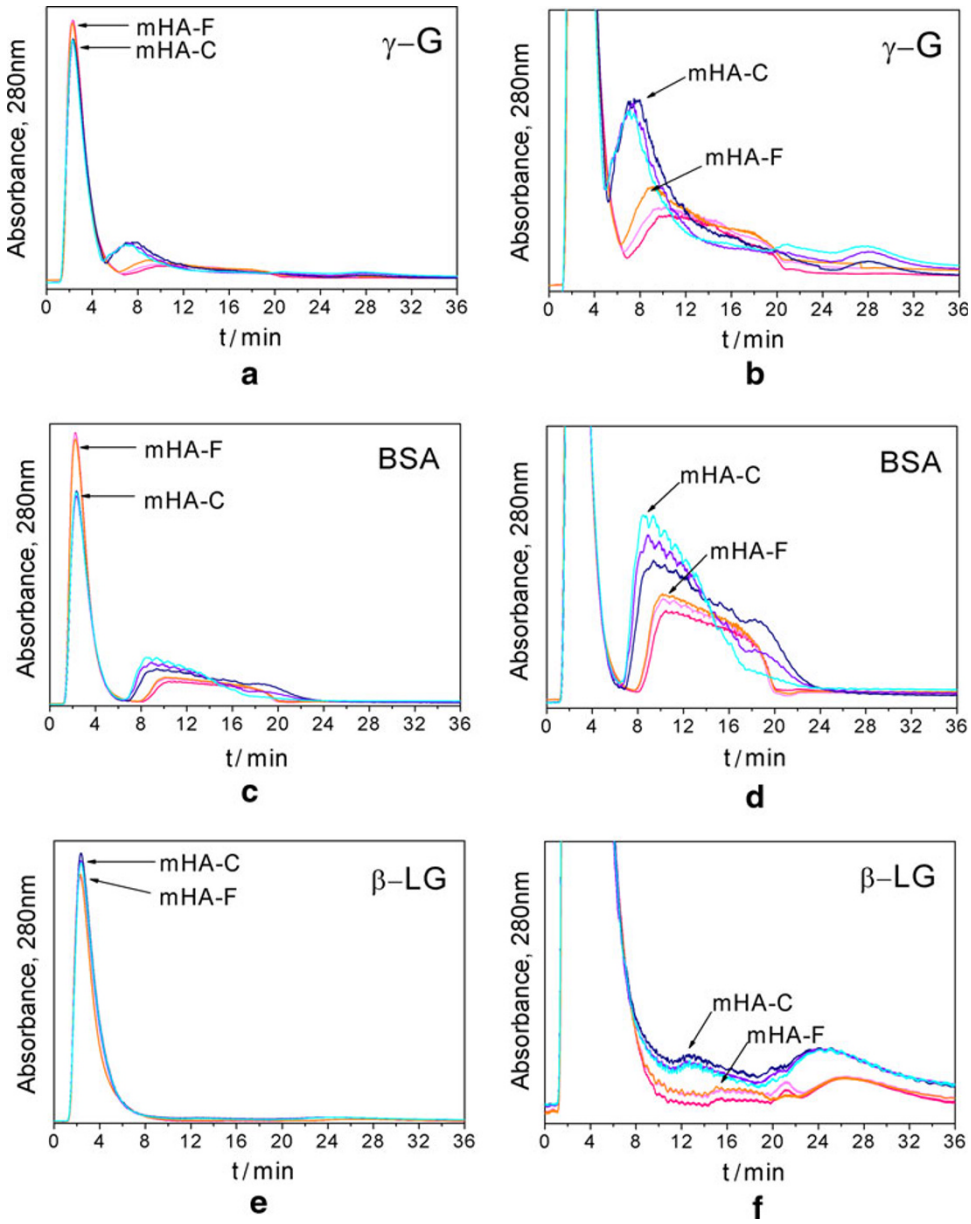

Fig. 4 Elution profile of γ-G, BSA and β-LG on mHA-C and mHA-F columns which were previously saturated with the corresponding protein. The *graphs* on the *right* (**b**, **d** and **f**) show the detail of the second elution *peak* observed from the **a**, **c** and **d** *plots* respectively

architectures support bone regeneration in the same way as not all materials are able to adsorb/absorb, retain and concentrate the proteins responsible for bone regeneration in the same manner. Retention and concentration denote, in the present work, those proteins that become entrapped in the structure of the material and, unlike ad/absorbed proteins, they are not physically bound. As mentioned earlier in the introduction, the gold standard procedure to validate osteoinduction against the multiscale architecture of materials is by in vivo implantation, but it becomes impractical and very expensive when various materials are to be tested. The results from SEC in the present work allow us to envisage the potential of this technique elucidating the effect of geometry at the nano/micro scale on the retention and concentration capability of proteins in the materials.

The materials of study were two HA scaffolds (mHA-C and mHA-F) with different architecture but an identical composition (Fig. 1) which closely mimicked that of bone and rendered the materials both, osteoconductive and bioactive [22]. The two scaffolds had very similar macroarchitecture consisting of a network of interconnected macropores but a markedly different architecture at the micro/nano level (Figs. 2, 3) [19]. Thus, the differences among both scaffolds resided in the wall of the scaffold. A denser network of needle-like crystal composed the wall of the mHA-F scaffold and a more open structure of needle/platy-like crystals that of the C scaffold (Fig. 3).

Table 1 Compilation of the protein elution doses (%), their corresponding elution times (expressed as the time it starts eluting till it finishes) and the protein elution span (Δt) for the two columns i.e., mHA-C and mHA-F

	C, elution (%)		F, elution (%)	
	1st peak	2nd peak	1st peak	2nd peak
γ-G	67.0 ± 2	31.0 ± 2.7	79.0 ± 6.7	21.0 ± 6.7
BSA	55.5 ± 1.3	44.2 ± 1.1	70.5 ± 1.5	29.0 ± 1.5
β-LG	78.6 ± 1.5	–	71.6 ± 0.2	–
	C, elution t (min)		F, elution t (min)	
	1st peak	2nd peak	1st peak	2nd peak
γ-G	1.2–4.7	3.8–13	1.2–4.7	5.6–20
BSA	1.2–4.5	7–18	1.2–4.5	8.3–20
β-LG	1.2–9.2	11.7–18.7	1.2–9.2	14.3–19.9
	C, elution Δt (min)		F, elution Δt (min)	
	1st peak	2nd peak	1st peak	2nd peak
γ-G	3.5	9.2	3.5	14.4
BSA	3.3	11	3.3	11.7
β-LG	8	7	8	5.6

– Too low content

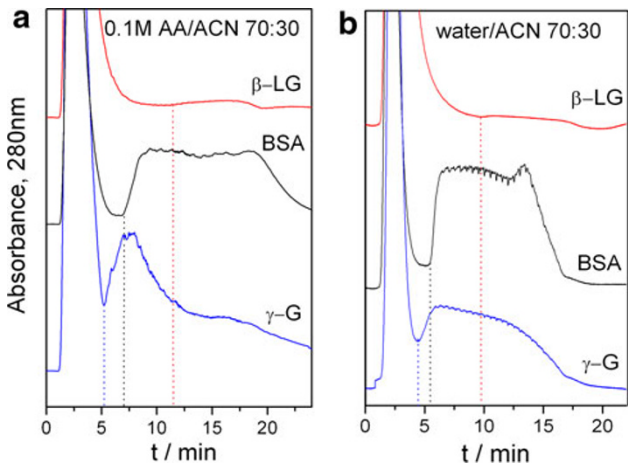

Fig. 5 Elution profile of γ-G, BSA and β-LG from mHA-C columns using two different mobile phases: **a** 70:30 v/v 0.1 M AA/ACN and **b** 70:30 v/v Milli Q water/ACN. The concentration of protein injected was 10 mg/ml in (**a**) and 3 mg/ml in (**b**)

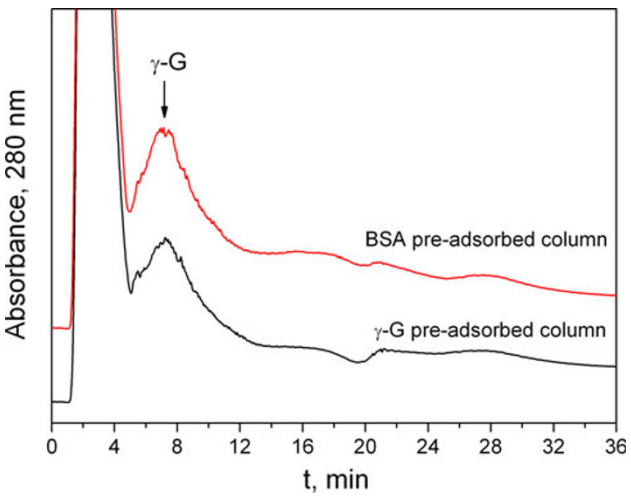

Fig. 6 Elution profile of γ-G from the mHA-C column previously saturated with either BSA or γ-G

One important aspect to note is that the range of microporosity found in the materials with pores below 0.1 μm (Fig. 3), was comparable to the size range of the proteins in blood. Fibrinogen for instance which is an abundant protein in blood has a rod-like shape and measures 46 nm in length [23]. Thus, if both materials were to be implanted, blood would flow through them and their specific microstructure would act as a sieve discriminating among proteins thus leading to a specific protein adsorption, retention and concentration pattern. Assessing the protein adsorption pattern is probably more straightforward than investigating the latter two and, in fact, the understanding that we have today on protein adsorption mechanisms on hydroxyapatite (HA) accounts for that [24–27]. This contrasts with the lack of reports focused on protein retention and concentration capability in 3D scaffolds for bone regeneration applications. Interestingly, size-exclusion chromatography is a chromatographic method which emerged as molecular sieve and, though used for different purposes, their results bear information on retention/concentration characteristics of a material.

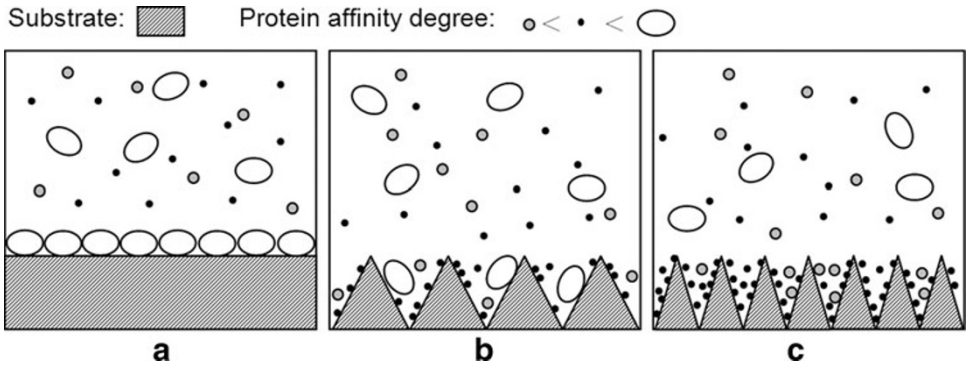

Fig. 7 Sketch depicting the role of texture in a material with regards to the adsorption and retention of proteins. It is assumed the continuous flushing of a mixture of proteins at the surface of a material. Proteins have different sizes, relative concentrations and affinities for the substrate. It is clearly observed that in spite of the fact that the protein in white colour has greater affinity for the substrate **a** the particular topography of the material might reduce **b** and even impede **c** its adsorption. Furthermore, textures presenting constricted spaces favour protein entrapment rendering, in turn, surfaces with a high content of entrapped/retained proteins (**b** and **c**)

Strictly speaking, the basis of ideal SEC assumes that there is no interaction between the solute, in our case the protein/s, and the stationary phase i.e. the material, and therefore implies that all the proteins must elute within the time required to renew the mobile phase that fully fills the voids of the column, i.e. void volume [28]. The capacity of a column (void volume) becomes then a critical factor in the visualization of the various exclusion events. Columns with too low capacity might not allow discriminating separately the various exclusion events as proteins would not have sufficient time to diffuse within the small pores of the column before elution and columns with too high capacity would result in long analysis times. In the present work, the difficulties of preparing large amount of macroporous material in a reproducible manner restricted the size of the columns to a specific amount of material insufficient to independently discriminate the various exclusion events. Moreover, the well known affinity of proteins towards HA further complicates visualization of exclusion events. Thus, to overcome these difficulties a particular strategy was developed. Before protein injection, the stationary phase was 1st pre-adsorbed with the protein of interest to saturate all binding sites of HA so as to facilitate exclusion events and 2nd, following column saturation, a rinsing cycle with ACN was applied in order to selectively enrich the smaller pores of the columns with ACN. The lower viscosity of ACN as compared to that of the mobile phase (30:70 v/v mixture of ACN with Milli Q water) was believed to facilitate protein diffusion into the pores thus allowing their separation. To confirm that this latter strategy was not altering the mechanism of interaction of the proteins with the column and that size exclusion was the main mechanism of interaction, experiments using mobile phases with various ionic strengths were performed (Fig. 5). In the case that a change in ionic strength modifies the protein elution profile this would be indicative of an affinity type of interaction mechanism between protein-column but if no alteration occurs then the main interaction mechanism would be of size-exclusion nature. The elution of the various proteins in mixtures of ACN with either Milli Q water or 0.1 M AA yielded similar protein elution profiles and elution order thus confirming that the main mechanism of interaction was indeed size exclusion. Nevertheless, in spite of the similar general appearance between chromatograms, there were some differences in the elution of BSA and γ-G in the two mobile phases which should not be misunderstood as other types of elution mechanisms but are simply the result of contribution of the blank (fraction of protein eluted owing to the rinsing process) in the chromatograms. Although the blank was usually subtracted in the various chromatograms (e.g. Figs. 4, 6), that was not the case in Fig. 5 which explains the alteration of the tail for the second elution peak in the results. Thus, if we obviate the contribution from the blank, the similarity among chromatograms improves, further supporting a separation mechanism mainly based on exclusion events. Similar differences were also detected in Fig. 4d in the mHA-C column regardless of subtraction of the blank. In this case the differences arose from subtracting the same blank in a series of independent runs instead of performing a blank per run. A separate experiment that was also done to corroborate the exclusion nature mechanism of interaction was to assess the elution of γ-G on a column pre-adsorbed with either BSA or γ-G (Fig. 6). Since there were no differences in the eluted profile which could point to an affinity type of interaction of γ-G with the scaffold, the results supported once again the exclusion nature of the separation events.

To better understand the contribution of SEC in this work, it is worth comparing the SEC chromatograms with the MIP plot (Figs. 3, 4). One seems the mirror image of the other as gauged by the presence of two peaks, one

sharper and of higher intensity than the other. This similarity is just a reflection of how tightly is linked one graph with the other. We can picture the mHA material (SEC column) as having an interconnected path of 80 μm width whereby proteins travelling through the main stream would quickly cross the column eluting first and, the proteins in contact with the material would be more or less entertained depending on the microarchitecture of the stationary phase thus eluting second. Since the size of the proteins (i.e. a few nanometers) is much inferior to the size of the interconnected macropores (10–200 μm), this will cause all proteins travelling through the main stream to elute at the same time. It is then not surprising to see that both columns with similar macroarchitecture have the first elution peak appearing at the same time. It is worth noting that proteins travelling this path become irrelevant to the material as they are simply excluded without allowing any kind of interaction. Depending on the type of column and protein, the amount excluded can vary from 60 % to almost 80 % of the injected amount (Table 1).

More interesting than investigating this first exclusion peak is to focus at the proteins travelling in contact with the stationary phase as they can potentially interact with the material. With regards to these proteins, and independent of any enthalpic interaction protein-material, it is clear that the proteins can diffuse differently into the pores affecting their retention time and their concentration capability. It is this type of events that become critical in order to understand the enhanced biological performance observed in certain materials and more specifically for certain geometries [7–10]. Differences in the microarchitecture between the F and C column resulted, indeed, in differences in the concentration and retention capability of the proteins as revealed from the second elution peak. The wall structure of the mHA-F scaffold, consisting in a denser network of smaller crystallites than for the C one, increased the retention time of the proteins (higher dwelling time) and decreased the protein concentration capability owing to the reduced space in between crystals. This trend though, was clearly observed for the BSA and γ-G proteins but became less obvious for the β-LG. We believe that was caused by an unexpected strong interaction of the protein with the material which caused β-LG to irreversibly adsorb onto the material rather than to delay its elution (30–40 % of the injected amount became adsorbed). Nevertheless the elution pattern for the β-LG can still be distinguished as shown in Fig. 4f. Another aspect to highlight is that the elution of each protein depended on their size, thus γ-G ($\sim$150 kDa), which is the largest, elutes first, BSA ($\sim$66 kDa) second and the smallest β-LG ($\sim$18 kDa) third. This trend was to be expected as the mechanism that prevails is entropically driven. Looking at the quantitative values gathered in Table 1 it is remarkable the amounts of proteins retained per protein and column. Thus, up to a 40 % of the injected BSA was retained in the C column while only a 25 % for the F one. In the case of γ-G practically the same amount than BSA was retained in F and only a 30 % in the C column.

The different behaviour shown in the amount retained per column demonstrates that it is possible to implement classic processing routes with simple characterization techniques to modulate the retention capability of a material. Understanding which proteins are retained and their specific amount (dose) is particularly important from various points of view. On the one hand we cannot overlook the fact that topography can involve the concentration/retention of large amounts of specific proteins (this will depend on the particular geometry of the material) which apart from 'hindering' the ad/absorbed surface might end up governing the nature of the ad/absorbed layer. If we also take into account that biological events are not restricted to ad/absorbed proteins but can also be triggered by concentration gradients, both, the bound and unbound 'protein states' have to be controlled to predict the response of the material. In addition, is worth noting that topography can override the intrinsic affinity of proteins for a substrate by simply acting as a sieve (please refer to the sketch in Fig. 7). Understanding and controlling these effects which have clearly been observed to play an important role in events like osteoinduction, blood clotting and cell function in general [2, 3, 29] have become an ongoing challenging field of investigation.

In spite of the 'apparent' distortion that topography causes on the nature of the protein layer at the surface of the material, we can take advantage of the sieving and concentrating capability of topography to design materials able to self-concentrate targeted proteins from the body (e.g. BMPs) instead of current approaches which use carriers for the delivery of a particular protein [29–31]. Quantifying and distinguishing this retained amount from what is adsorbed is also critical because it affects the mechanism by which the biomaterial influences a biological function [29].

Thus, this study which in essence has been performed minimising any enthalpic interaction, has given a good account on how via entropic mechanisms the different proteins are able to discriminate the micro/nanoarchitecture created by the entanglement of crystals of different sizes (F vs. C). Nevertheless, it is important to bear in mind that the present study only gives a partial view as in an in vivo situation both, entropic and enthalpic interactions would always occur. The immediate goal following this work will be the preparation of columns with greater dimensions so that the different exclusion events along with any enthalpic event would be readily observed using a mobile phase similar to physiological conditions. In fact, one concern in

the present work was the effect that organic solvents like ACN might have caused on the protein conformation and elution profile albeit its content in the mobile phase was kept low enough to minimize any changes [32]. This is a problem though, that is readily solved working with larger columns as the requirement of using ACN to favor protein diffusion into the pores would no longer be needed. Under those conditions, the injection of complex protein mixtures could then be made and fractions of the eluate could be retrieved to further analyse its content. We believe that SEC can become a powerful tool characterizing constructs to be applied in the tissue engineering field.

5 Conclusions

Size-exclusion chromatography has proved to be a successful tool for the investigation of the concentration and entrapment behaviour of proteins in two different macroporous HA scaffolds (mHA) with similar macroarchitecture but different microarchitecture, i.e. mHA-C *versus* mHA-F. The larger size and lower density of entangled crystals in the C material as compared to the F one allowed for more protein concentration and a faster elution time. Furthermore, proteins with different sizes i.e., γ-G, BSA and β-LG, were shown to discriminate differently the microarchitecture created by both materials. This was observed in the different retention times and the amounts retained per column. We propose the use of SEC to screen the geometry of TE scaffolds in order to identify the best architecture that would enhance concentration/retention of proteins of interest.

Acknowledgments The authors thank Eva Maria del Alamo and Esther Miralles for technical assistance during SEC analysis. This work was funded by the European Commission through the ANGIOSCAFF project NMP3-LA-2008-214402 and the Spanish Ministry through the project MAT2009-13547. M.P. Ginebra also acknowledges funding from the Generalitat de Catalunya through the prize ICREA Academia for excellence in research.

References

1. Horbett TA (1982) In: Cooper SL, Peppas NA, Hoffman AS, Ratner BD (eds) Biomaterials: interfacial phenomena and applications. Advances in chemistry series. American Chemical Society, Washington DC
2. Roach P, Farrar D, Perry CC (2006) J Am Chem Soc 128:3939–3945
3. Lord MS, Foss M, Besenbacher F (2010) Nano Today 5:66–78
4. Lord MS, Cousins BG, Doherty PJ, Whitelock JM, Simmons A, Williams RL, Milthorpe BK (2006) Biomaterials 27:4856–4862
5. Vroman L, Adams AL, Fischer GC, Munoz PC, Standford M (1982) In: Cooper SL, Peppas NA, Hoffman AS, Ratner BD (eds) Biomaterials: interfacial phenomena and applications. American Chemical Society, Washington DC
6. Ripamonti U, Herbst NN, Ramoshebi LN (2005) Cytok Growth Factor Rev 16:357–368
7. Ripamonti U, Crooks J, Kirkbride AN (1999) S Afr J Sci 95:335–343
8. Habibovic P, Huipin Y, van der Valk CM, Meijer G, van Blitterswijk CA, de Groot K (2005) Biomaterials 26:3565–3575
9. Habibovic P, Sees TM, van den Doel M, van Blitterswijk CA, de Groot K (2006) J Biomed Mater Res 77A:747–762
10. LeGeros RZ (2008) Chem Rev 108:4742–4753
11. Yuan H, Fernandes H, Habibovic P, de Boer J, Barradas AMC, de Ruiter A, Walsh WR, van Blitterswijk A, de Bruijn JD (2010) Proc Natl Acad Sci USA 107:13614–13619
12. Irvine GB (1997) Anal Chim Acta 352:387–397
13. Barth HG, Boyes BE, Jackson C (1998) Anal Chem 70:251R–278R
14. Liang H, Scott MK, Murry DJ, Sowinski KM (2001) J Chromatogr B Anal Technol Biomed Life Sci 754:141–151
15. Kawasaki T, Takahashi S, Ikeda K (1985) Eur J Biochem 152:361–371
16. Grodzki AC, Berenstein E (2010) Methods Mol Biol 588:33–41
17. Neville B (1996) In: Doonan S (ed) Protein purification protocols methods in molecular biology. Humana Press Inc, Totowa
18. Mahn A, Lienqueo ME, Asenjo JA (2007) J Chromatogr B Anal Technol Biomed Life Sci 849:236–242
19. Espanol M, Perez RA, Montufar EB, Marichal C, Sacco A, Ginebra MP (2010) Acta Biomater 5:2752–2762
20. Montufar EB, Traykova T, Planell JA, Ginebra MP (2011) Mat Sci Eng C 31:1498–1504
21. Ginebra MP, Fernandez E, de Maeyer EAP, Verbeeck RMH, Boltong MG, Ginebra J, Driessens FCM, Planell JA (1997) J Dent Res 76:905–912
22. Hench LL, Polak JM (2002) Science 295:1014–1017
23. Hall CE, Slayter HS (1959) J Biophys Biochem Cytol 5:11–16
24. Kawasaki T (1991) J Chrom A 544:147–184
25. Yin G, Liu Z, Zhan J, Ding F, Yuan N (2002) Chem Eng J 87:181–186
26. Mura-Galelli MJ, Voegel JC, Behr S, Bres EF, Schaaf P (1991) Proc Natl Acad Sci USA 88:5557–5561
27. Barroug A, Lernoux E, Lemaitre J, Rouxhet PG (1998) J Coll Int Sci 208:147–152
28. Berek D (2010) J Sep Sci 33:315–335
29. Uludag H, Gao T, Porter TJ, Friess W, Wozney JM (2001) Delivery systems for BMPs: factors contributing to protein retention at an application site. J Bone Joint Surg 83A(1):128–135
30. Bessa PC, Casal M, Reis RL (2008) J Tissue Eng Regener Med 2:81–96
31. De Groot K (1998) Tissue Eng 4:337–341
32. Gekko K, Ohmae E, Kameyama K, Takagi T (1998) Biochim Biophys Acta 1387:195–205